JACS
JOURNAL OF THE AMERICAN CHEMICAL SOCIETY
Article
Cite This: J. Am. Chem. Soc. 2018, 140, 13726−13735
pubs.acs.org/JACS

Organocatalytic [6+4] Cycloadditions via Zwitterionic Intermediates: Chemo-, Regio-, and Stereoselectivities

Peiyuan Yu,[†,#] Cyndi Qixin He,[†,#] Adam Simon,[†] Wei Li,[†] Rasmus Mose,[§] Mathias Kirk Thøgersen,[§] Karl Anker Jørgensen,[§] and K. N. Houk*[,†,‡]

[†]Department of Chemistry and Biochemistry, and [‡]Department of Chemical and Biomolecular Engineering, University of California, Los Angeles, California 90095, United States

[§]Department of Chemistry, Aarhus University, DK-8000 Aarhus C, Denmark

Supporting Information

ABSTRACT: The mechanisms and origins of chemo- and stereoselectivities of the organocatalytic [6+4] cycloaddition between 2-cyclopentenone and tropone have been investigated by a combined computational and experimental study. In the presence of a cinchona alkaloid primary amine catalyst and an acid additive, 2-cyclopentenone forms a cross-dienamine intermediate that subsequently undergoes a stepwise [6+4] cycloaddition reaction via a zwitterionic intermediate. The rate-determining transition state features a strong hydrogen-bonding interaction between the tropone oxygen atom and the protonated quinuclidine directing the reaction course leading to a highly periselective [6+4] cycloaddition. The importance of the strong hydrogen-bonding interaction is also demonstrated by the influence of the concentration of the acid additive on the yields and enantioselectivities of the reaction. The corresponding [4+2] cycloaddition reaction has a much higher energy barrier. The enantioselectivity of the [6+4] cycloaddition originates from different repulsive hydrogen−hydrogen interactions that distinguish the diastereomeric transition states.

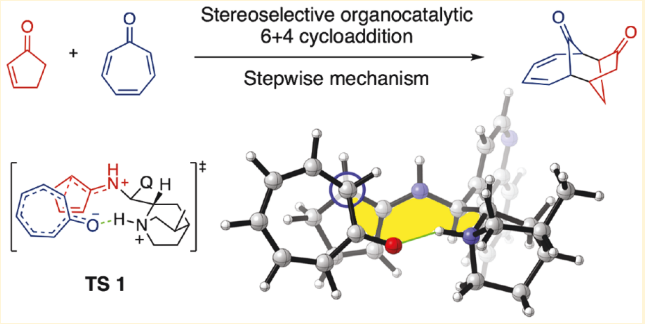

INTRODUCTION

Cycloaddition reactions are ubiquitous reactions in organic chemistry. Since the discoveries by Diels and Alder,[1] numerous synthetic applications,[2] and subsequent theoretical considerations by Woodward and Hoffmann,[3] Diels−Alder cycloaddition reactions have become standard methods for the construction of six-membered ring systems. The [4+2] cycloaddition involves six π-electrons, and all aspects of the different types of selectivity can, to a very high extent, be controlled by variation of substituent patterns, catalysis and reaction conditions.[4] The understanding of the reaction course of the [4+2] cycloadditions performed under a variety of reaction conditions has been the goal of numerous experimental and computational studies.[5]

Cycloadditions in which more than six π-electrons are involved have been called higher-order cycloadditions. Ten π-electron cycloadditions such as [6+4] and [8+2] cycloadditions are, compared to the [4+2] cycloadditions, less well known and more challenging to control.[6] These higher-order cycloadditions often suffer from lack of periselectivity, as many different pericyclic reactions may occur with extended π-systems. Tropone, for example, may act as a 2π-, 4π-, 6π- or 8π component in cycloadditions, depending on the reaction partner.[7] A further challenge for higher-order cycloadditions is to control the *exo*/*endo* stereoselectivity and enantioselectivity in the presence of a chiral catalyst. Regioselectivity provides yet another challenge. Being able to control peri- and stereoselectivity in higher-order cycloadditions would enable their use in the generation of complex natural product or drug targets.

Periselectivity and stereoselective control of higher-order cycloadditions has been described rarely; Rigby et al.[8] identified a metal-promoted intramolecular [6+4] cycloaddition reaction which proceeds in good yield and low enantioselectivity, while Feng et al. reported a metal-catalyzed *aza*-[8+2] cycloaddition.[9] Garst and Houk described examples and a model to rationalize regioselectivity in [6+4] cycloadditions of substituted dienes and tropones.[10]

Recently, the first example of stereoselective [6+4] and [8+2] cycloadditions catalyzed by cinchona alkaloid primary amines was disclosed (Scheme 1).[11] In addition to stereoselective catalysis, these reactions exhibited periselectivity that could be tuned by varying the ring size of the cyclic enones and altering the substitution patterns of the tropone/heptafulvenes.

We have now carried out combined computational and experimental studies of the factors that govern the reaction pathways for higher-order [6+4] cycloaddition reactions, concentrating first on the reaction of cyclopentenone, **1**, and tropone, **2**. We report computational and additional experimental

Received: July 18, 2018
Published: September 25, 2018

DOI: 10.1021/jacs.8b07575
J. Am. Chem. Soc. 2018, 140, 13726−13735

Scheme 1. Peri- and Stereoselective Cycloadditions by Cinchona Alkaloid Primary Amine Catalysts

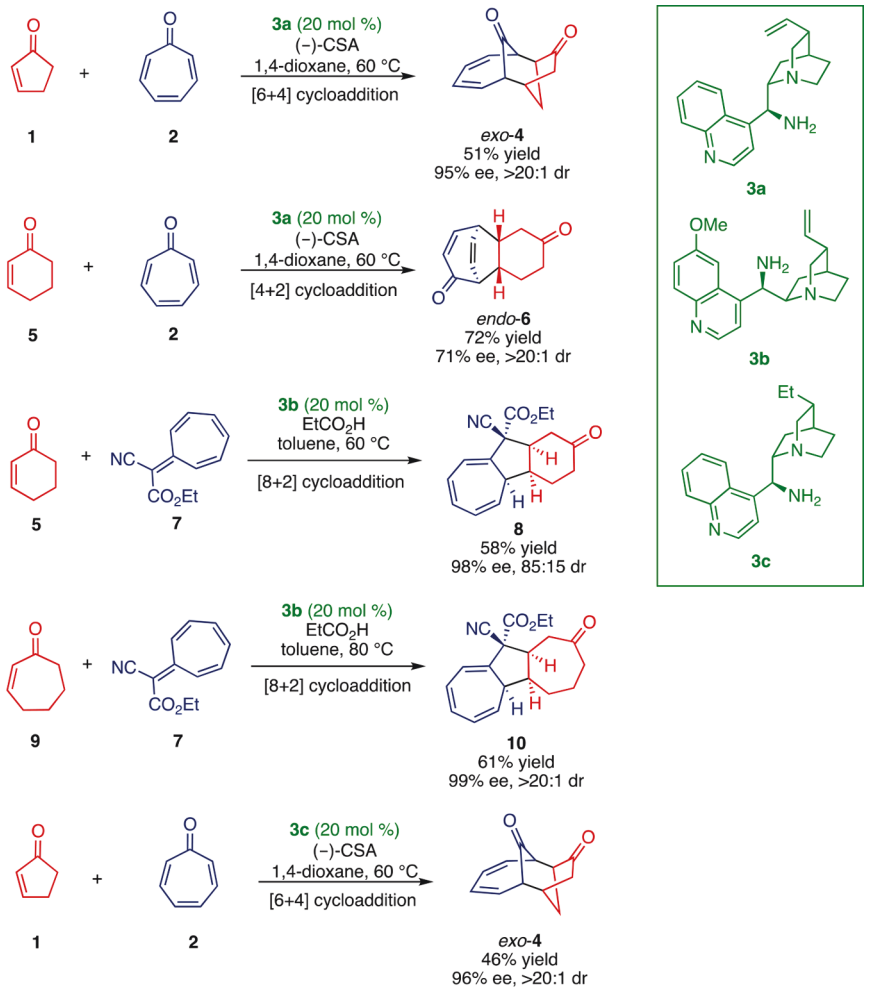

investigations of (1) the periselectivity of the plausible cycloadditions between the dienamine intermediate(s) formed from 2-cyclopentenone and a cinchona alkaloid primary amine catalyst, and tropone, and (2) the diastereo- and enantioselectivities of the [6+4] cycloaddition.

COMPUTATIONAL METHODS

Quantum mechanical computations were performed using Gaussian 09.[12] The geometries were fully optimized at the B3LYP[13]/6-31G(d) level of theory with the SMD implicit solvation model[14] to account for the solvation effects of 1,4-dioxane, the solvent used in the experiments. All of the optimized geometries were verified by frequency computations as minima (zero imaginary frequencies) or transition structures (a single imaginary frequency). Single-point energies of the optimized geometries were evaluated using the more accurate density functional M06-2X[15] and the larger 6-311+G(d,p) basis set. The thermal corrections evaluated from the unscaled vibrational frequencies at the B3LYP/6-31G(d) level on the optimized geometries were then added to the M06-2X/6-311+G(d,p) electronic energies to obtain the free energies. The free energies were corrected using Truhlar's quasiharmonic correction, by raising vibrational frequencies that are below 100 cm^{-1} to 100 cm^{-1}.[16] Reaction barriers and selectivities computed from different density functionals and basis sets were also compared to ensure that reported results are consistent using different methods.

RESULTS AND DISCUSSION

The reaction of 2-cyclopentenone **1** with tropone **2** in the presence of the cinchona alkaloid primary amine catalyst **3a** proceeds via a cross-dienamine intermediate. We began our investigation by comparing the computed relative stabilities of cross- and linear-dienamine intermediates. The results are shown in Figure 1.

The formation of dienamines from 2-cyclopentenone **1** and a simple *N*-methylamine is endergonic by ∼4 kcal/mol. The cross-dienamine intermediate **11** is slightly less stable than the linear-dienamine intermediate **12** by 0.4 kcal/mol (Figure 1A). For comparison, this difference is larger (2.1 kcal/mol) in the acyclic system (Figure 1B), and this linearly conjugated system is most stable. In the presence of the cinchona alkaloid primary amine catalyst under acidic conditions present in these reactions, the cross-dienamine intermediate **15** is more stable than the linear-dienamine intermediate **16** by 2.2 kcal/mol (Figure 1C). Our computational model catalyst is protonated at the quinuclidine nitrogen atom and contains a truncation of the vinyl group in catalyst **3a** to a methyl group to reduce conformational complexity. The truncation is a reasonable approximation, as experimental results have shown the [6+4] cycloaddition between 2-cyclopentenone **1** and tropone **2** catalyzed by **3c**, in which the vinyl group of **3a** is reduced to an ethyl group, give similar results as for catalyst **3a** (Scheme 1).

We next explored the mechanism of the [6+4] cycloaddition between model cross-dienamine intermediate **11** and tropone **2**. It was found that the [6+4] cycloaddition is a stepwise process (Figure S1 of the Supporting Information). The pericyclic processes, known for cyclopentadiene or dimethylfulvene

DOI: 10.1021/jacs.8b07575
J. Am. Chem. Soc. 2018, 140, 13726−13735

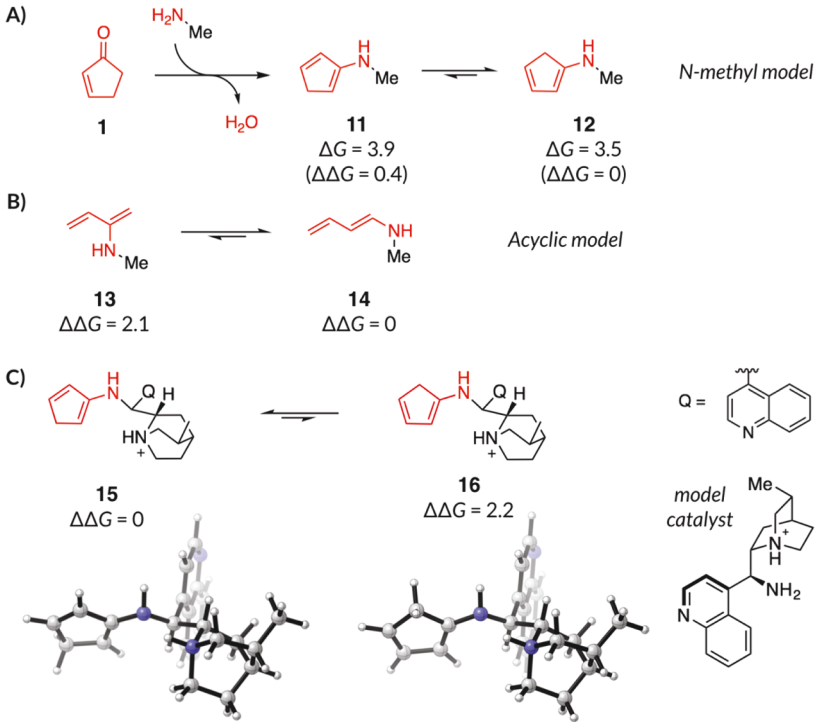

Figure 1. Relative stabilities of different cross- and linear-dienamine intermediates. All energies are in kcal/mol.

as dienes[7,17] become stepwise, polar intermediate cycloadditions with the dienamines as 4π-reactants.

The FMOs of the nucleophilic diene and the relatively electrophilic tropone are shown in Figure 2. The HOMO of the diene is strongly polarized toward C-1, and the terminal coefficients at C-1 and C-4 are very different in magnitude, accounting for the tendency of this diene to react in a stepwise fashion. C-1 becomes bonded to C-2 of tropone, which has the largest LUMO coefficient. While C-4 has nearly as large a LUMO coefficient, interaction of a nucleophile at this position suffers significant antibonding secondary interaction with C-5.

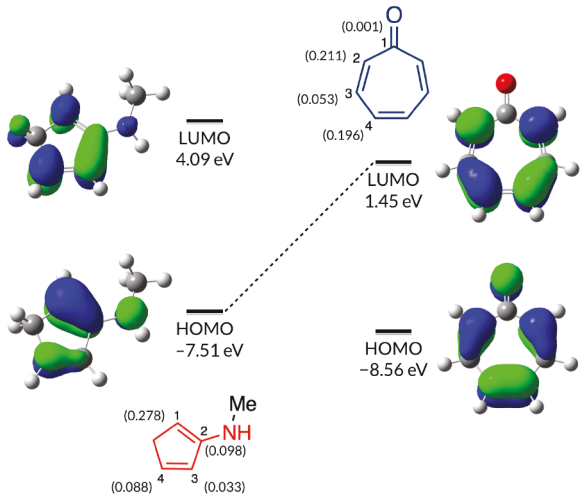

Figure 2. Computed FMOs of *N*-methyl cross-dienamine intermediate **11** and tropone **2**. HF/6-31G(d) is used for the computation of the FMOs on DFT-optimized structures. Numbers in parentheses are sums of squares of the HOMO (dienamine) or LUMO (tropone) coefficients at the corresponding carbon atoms.

We also explored other potential modes of reaction, the attack of the diene C-1 at tropone C-3 or C-4. These transition states are higher in energy by 11.2 and 4.8 kcal/mol, respectively (see Supporting Information).

There are three possible staggered conformations about the first C−C bond in the transition-state (TS) structures for a stepwise process (Figure 3A). In addition, the *N*-methyl moiety of the cross-dienamine intermediate **11** can adopt either *s-cis* or *s-trans* conformation (Figure 3B). Thus, a total of six TS structures were located for the first step of the *exo*-[6+4] cycloaddition between cross-dienamine intermediate **11** and tropone **2**.

Figure 3C shows a total of six TS structures corresponding to the three staggered conformers about the C−C forming bond and the two conformers about the C−N single bond. Overall, the *s-trans* TS conformers (Figure 3C, top) are more stable than the *s-cis* conformers (Figure 3C, bottom). Within the *s-trans* TS conformers, the two *gauche*-TSs **17a** and **17b** are lower in energy than the *anti*-TS **17c**, which follows Seebach's topological rule for carbon−carbon bond formation due to maximization of electrostatic attraction between developing partial charges.[18] TS structure **17a** is the most stable, due to the proximity of the developing positive and negative charges. In this TS, the distance between the carbonyl oxygen atom and hydrogen atom with most positive charge is 2.41 Å, both **17a** and **17b** have stabilizing secondary orbital interactions of the [6+4] type, either 4π enamine plus 6π tropone, or 4π diene plus 6π tropone. The higher energy, **17c** and **18c**, have no such secondary orbital interactions.

Similarly, there are six TSs for the *endo*-[6+4] cycloaddition between the cross-dienamine intermediate **11** and tropone **2** and 12 TSs for the [6+4] cycloaddition between the linear-dienamine intermediate **12** and tropone **2**. They are higher in energy than TS **17a** by at least 2.6 kcal/mol. These results are summarized in Figure S2 of the Supporting Information.

We next expanded the computational model to explore the more flexible conformations of the [6+4] cycloaddition TS in

DOI: 10.1021/jacs.8b07575
J. Am. Chem. Soc. 2018, 140, 13726−13735

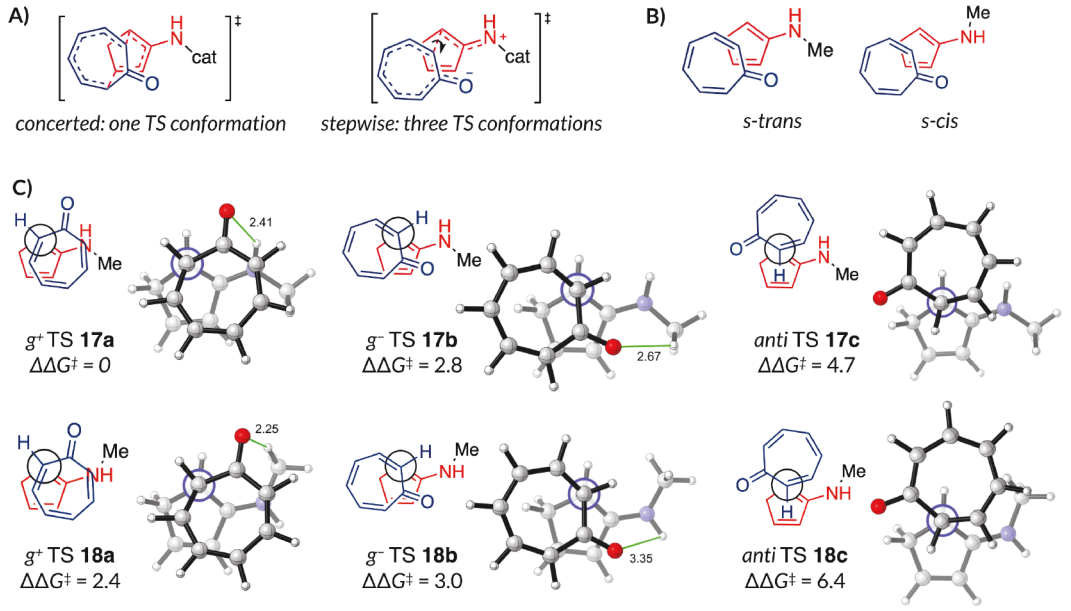

Figure 3. Transition structures of a simplified *N*-methyl cross-dienamine intermediate model. *Gauche* describes the relative position of the carbonyl carbon and the nitrogen-bearing carbon. All energies are in kcal/mol. Distances are in Å.

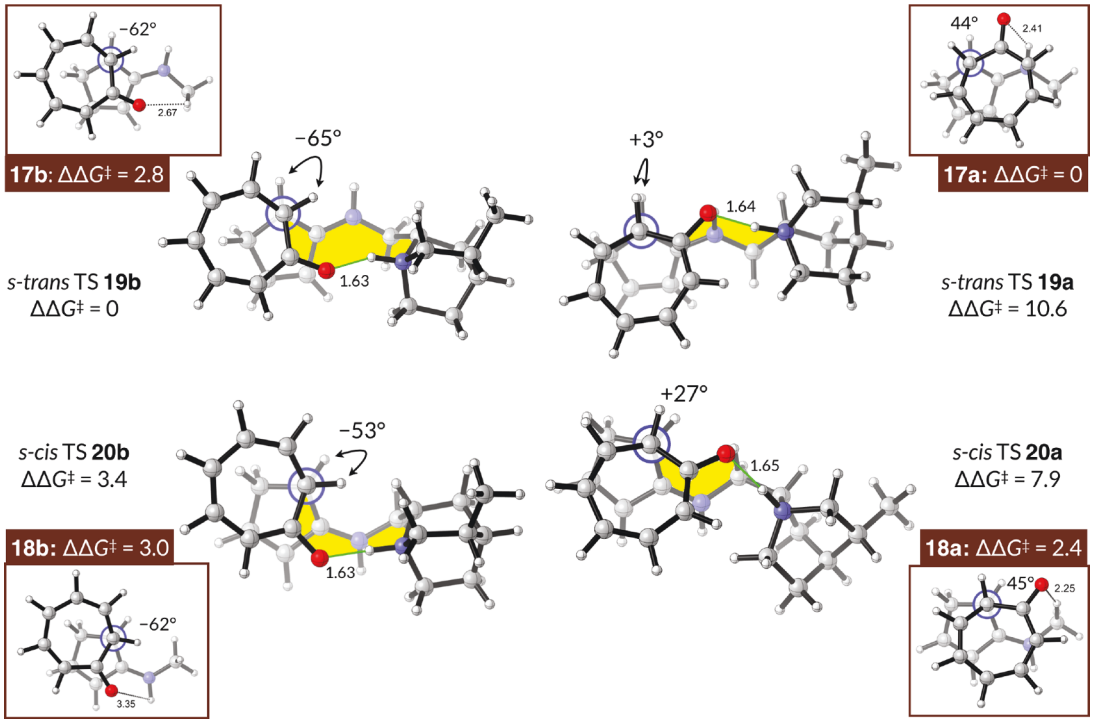

Figure 4. Transition structures of the quinoline-truncation model. For comparison, the corresponding *N*-methyl model TSs are shown in the brown boxes. All energies are in kcal/mol. Distances are in Å.

the presence of a catalyst with a quinuclidinium moiety (**3a** without the quinoline substituent). As shown in Figure 4, the tropone oxygen atom now forms a hydrogen bond with the protonated quinuclidine, and the carbon−carbon bond-forming TS features a 9-membered macrocycle excluding the hydrogen (colored in yellow). The *anti*-conformation about the forming C−C bond cannot be adopted in this model. TS structures **19a,b** and **20a,b** are built on the *gauche*-conformers in the *N*-methyl cross-dienamine intermediate model shown in Figure 3C (also shown in the brown boxes in Figure 4 for comparison).

While TS **17a** in the *N*-methyl model is the lowest energy TS conformer, the corresponding TS **19a** is substantially higher in energy ($\Delta\Delta G^{\ddagger}$ = 10.6 kcal/mol) than TS **19b**. This is due to the ideal electrostatic and secondary orbital arrangement in **17a** and **18a** which cannot be achieved while maintaining the O---HN^{+} hydrogen bond (see Supporting Information for a detailed analysis). The *gauche*-(−) TS conformation is unachievable in the presence of the quinuclidinium ring, and instead, the eclipsed conformation has to be adopted. TSs **20a** and **20b**, with the *s-cis* cross-dienamine intermediate are also higher in energy. The lowest-energy TS conformer **19b** features

DOI: 10.1021/jacs.8b07575
J. Am. Chem. Soc. 2018, 140, 13726−13735

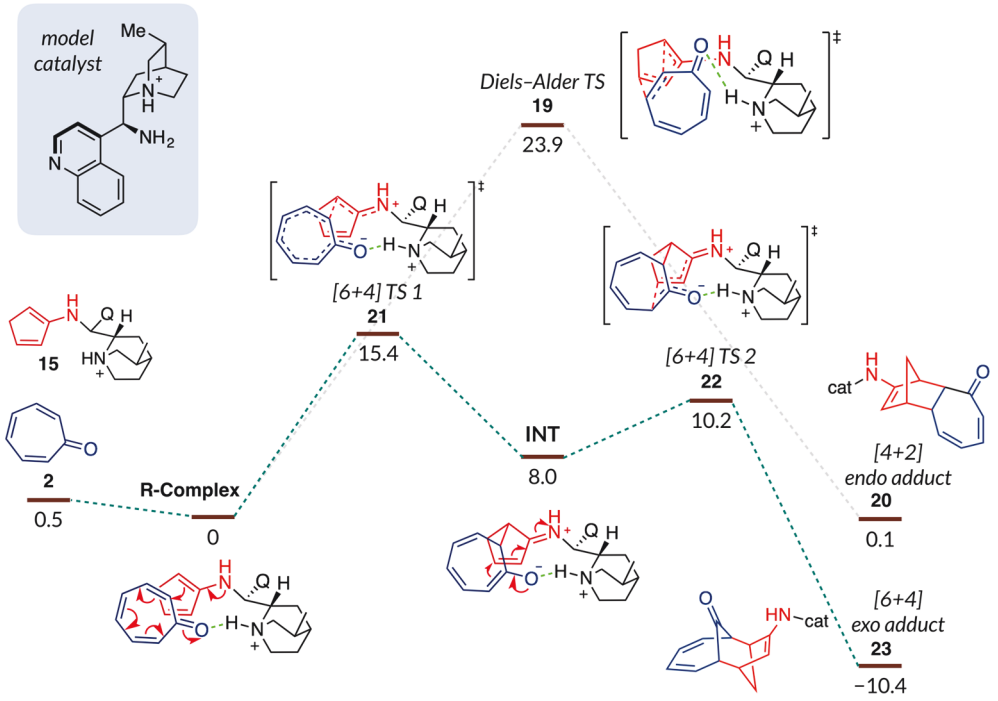

Figure 5. Free energy profile of the [6+4] and [4+2] cycloadditions between tropone **2** and cross-dienamine intermediate **15**. All energies are in kcal/mol.

Scheme 2. Reaction Supporting a Stepwise Mechanism for the Reaction of 2-Cyclopentenone 1 with Tropone 2[a]

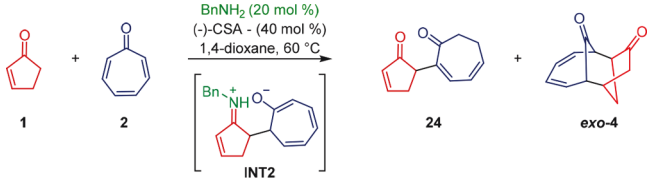

[a]For experimental details, see Supporting Information

the *gauche*-(+) conformation about the forming C–C bond as well as a crown-like conformation of the macrocycle.

Finally, we expanded our analysis to include the quinoline substituent on cross-dienamine intermediate **15**. The lowest energy pathways of the possible [6+4] and [4+2] cycloadditions of tropone and cross-dienamine intermediate **15** are depicted in Figure 5.

The cross-dienamine intermediate **15**, formed from 2-cyclopentenone **1** and the model catalyst, can react with tropone **2** to undergo [6+4], [4+2], or [8+2] cycloadditions. Our results show that the Diels–Alder [4+2] pathway via concerted TS **19** is 8.5 kcal/mol higher in energy than the stepwise [6+4] pathway, in accordance with the relative stabilities of the corresponding products. The [8+2] pathway is endergonic (not shown). The most favorable pathway leads to the [6+4] adduct, which is consistent with the high periselectivity observed experimentally. The rate-determining step is the first C–C bond formation via **21** and has a barrier of 15.4 kcal/mol. The

Scheme 3. Role of the Stereochemistry of the Anionic Counterion for the Reaction of 2-Cyclopentenone 1 with Tropone 2 in the Presence of the Cinchona Alkaloid Primary Amine Catalyst 3a[a]

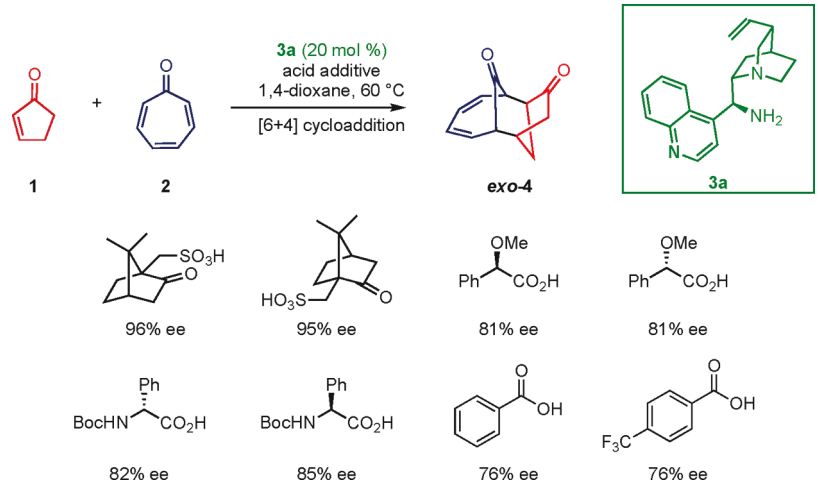

[a]For experimental details, see Supporting Information.

DOI: 10.1021/jacs.8b07575
J. Am. Chem. Soc. 2018, 140, 13726–13735

Table 1. Influence of (−)-CSA Concentration on the Conversion (Yield) and Enantiomeric Excess of the Reaction of 2-Cyclopentenone 1 with Tropone 2 in the Presence of the Cinchona Alkaloid Primary Amines Catalyst 3a[a]

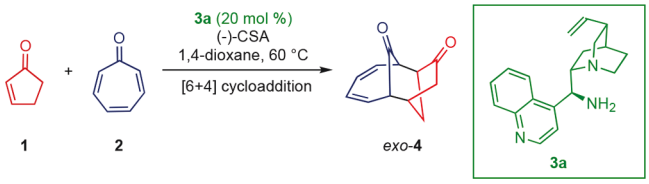

entry	(−)-CSA (mol%)	conversion (yield) (%)	ee (%)
1	10	27 (22)	62
2	20	42 (22)	92
3	30	65 (44)	95
4	40	92 (58)	95
5	50	97 (53)	91

[a]For experimental details, see Supporting Information.

zwitterionic intermediate is only 8 kcal/mol above the reactants. The second TS is lower in energy than the first TS by about 5 kcal/mol. The lowest energy TS **21** adopts a conformation that is similar to TS **19b** in Figure 4. The aforementioned secondary orbital interaction of the [6+4] sense in **21** becomes the second bond formed in the second TS **22**. The TS structures arising from the less stable linear-dienamine intermediate **16** are at least 4 kcal/mol higher in energy than the ones from **15** (Figure S5 in the Supporting Information).

The computed stepwise mechanism of the [6+4] cycloaddition reaction is supported by a non-cyclized byproduct **24** found when benzylamine is used as organocatalyst under the standard reaction conditions (Scheme 2). Benzylamine does not possess the dual-activation properties offered by **3a**, and slower conversion of the intermediate **INT2** to the [6+4] cycloadduct *exo*-**4** results in partial hydrolysis of the intermediate **INT2** followed by tautomerization to **24**. The non-cyclized byproduct **24** has not been observed when the reaction was catalyzed by **3a**, which underlines the importance of the dual catalytic properties of **3a**.

The importance of hydrogen bonding in the cyclic TS structure (as shown in Figure 5), inspired us to pursue further investigations of the role of the stereochemistry of acid on the periselectivity of the [6+4] cycloaddition. The role of the anionic counterion was studied experimentally by employing a series chiral acid pairs in the reaction between 2-cyclopentenone **1** and tropone **2** catalyzed by cinchona alkaloid primary amine catalyst **3a** (Scheme 3). The results in Scheme 3 shows that the stereochemical outcome of the reaction is independent of the stereochemistry of the chiral counteranion; e.g., the reactions performed with each enantiomer of CSA result in the same enantiomer of the product *exo*-**4** with similar enantioselectivity. Comparable results are obtained for the two other chiral acids investigated, although there are minor changes in enantioselectivity (81−96% ee) between respective pairs of acids.

The stereochemical outcomes of reactions in the presence of achiral organic acids, commonly used as additives in organocatalysis, such as benzoic acid and *p*-trifluorobenzoic acid, have also been investigated under the same reaction conditions as in Scheme 3. For both benzoic acid and *p*-trifluoromethylbenzoic acid, the enantioselectivity of *exo*-**4** was measured as 76% ee. Reactions performed with a variety of *para*-substituted benzoic acid derivatives in toluene as the solvent also demonstrated a very limited effect of the achiral counterion (for further details and examples, see Supporting Information).

The absence of matched/mismatched interactions for the reactions with pairs of chiral acid additive demonstrates a minor importance of the counterion on the reaction. Therefore, we conclude that it is reasonable to exclude the anionic counterion from the calculations of the reaction pathway.

Next, the influence of the amount of acid additive was investigated experimentally. A series of reactions was performed in which 10, 20, 30, 40, and 50 mol% (−)-CSA was present in the reaction mixture (Table 1).

The results in Table 1 show that the conversion of tropone **2** and the yield and enantiomeric excess of *exo*-**4** to a certain extent are dependent on the amount of (−)-CSA present. For the conversion to proceed to >90%, 40 mol% of (−)-CSA is required. At the lowest concentration of (−)-CSA, *exo*-**4** is obtained with 62% ee, while the reaction in the presence of

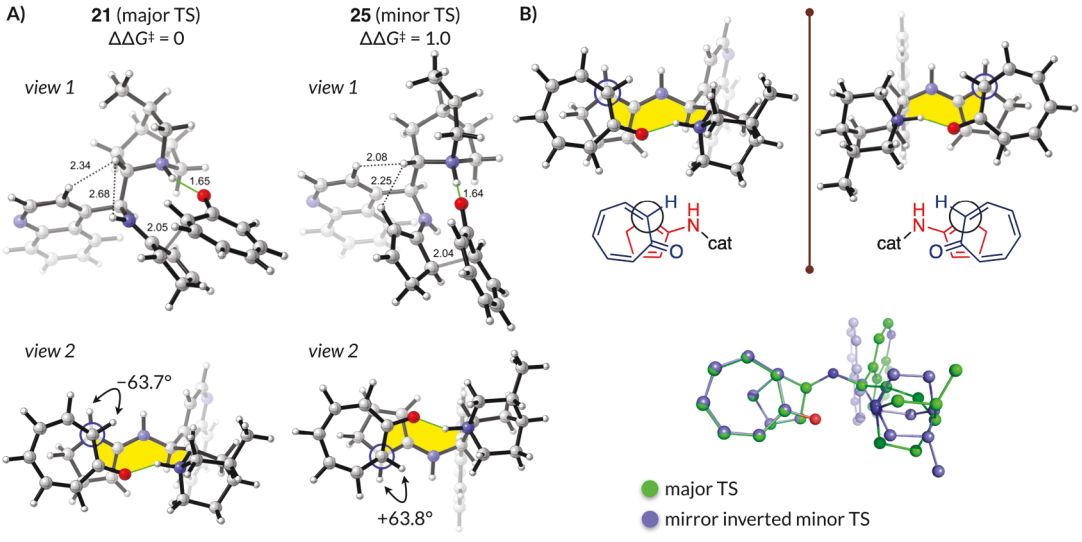

Figure 6. (A) Stereo-determining TS structures of the formal [6+4] reaction. (B) Overlay of the major and the mirror inverted minor TS structure. All energies are in kcal/mol. Distances are in Å.

DOI: 10.1021/jacs.8b07575
J. Am. Chem. Soc. 2018, 140, 13726−13735

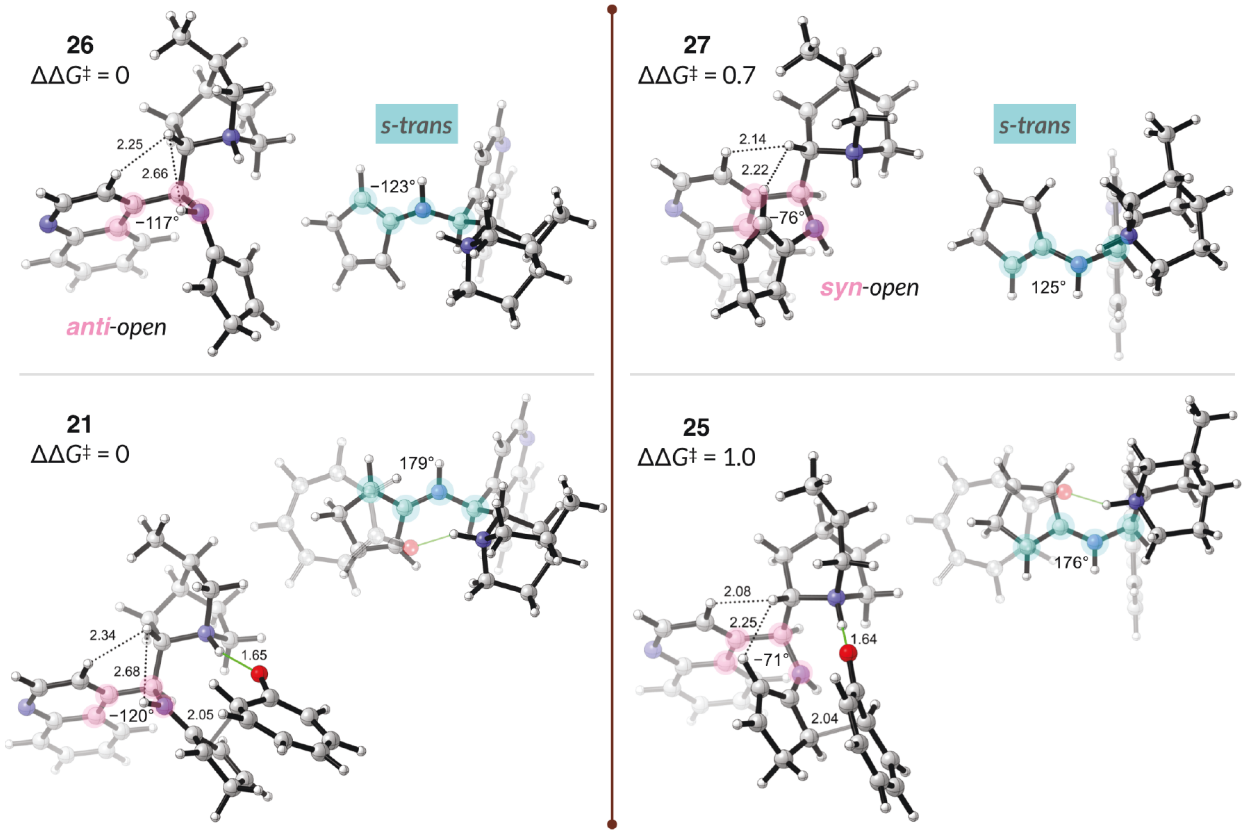

Figure 7. Energetics of chiral dienamine intermediate conformers. All energies are in kcal/mol. Distances are in Å.

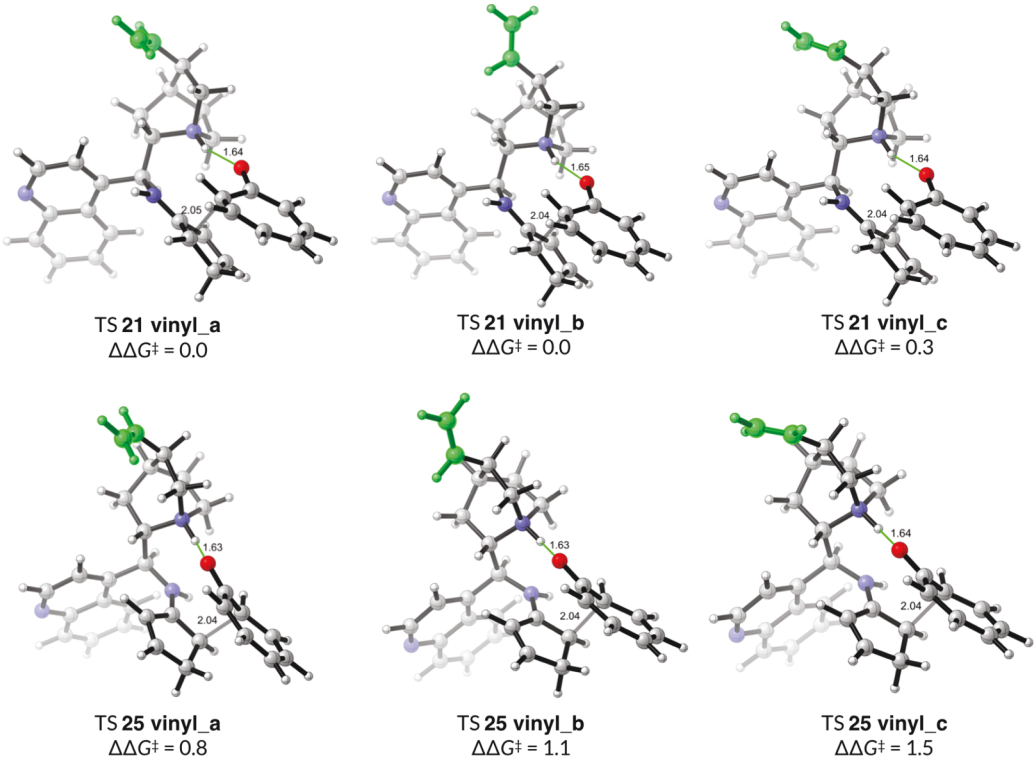

Figure 8. Enantio-determining TS structures using exact catalyst model with the vinyl group. All energies are in kcal/mol. Distances are in Å.

20 mol% (−)-CSA gives 92% ee, a result which is not changed at higher concentrations of (−)-CSA. These results are consistent with the calculated reaction pathway, as the equilibrium between the acid and the quinuclidine base determines the reaction rate through the concentration of active protonated catalyst and that the quinuclidine has to be protonated in order to obtain high yields and enantioselectivity. At low concentrations of (−)-CSA the reaction might also proceed through a

DOI: 10.1021/jacs.8b07575
J. Am. Chem. Soc. 2018, 140, 13726−13735

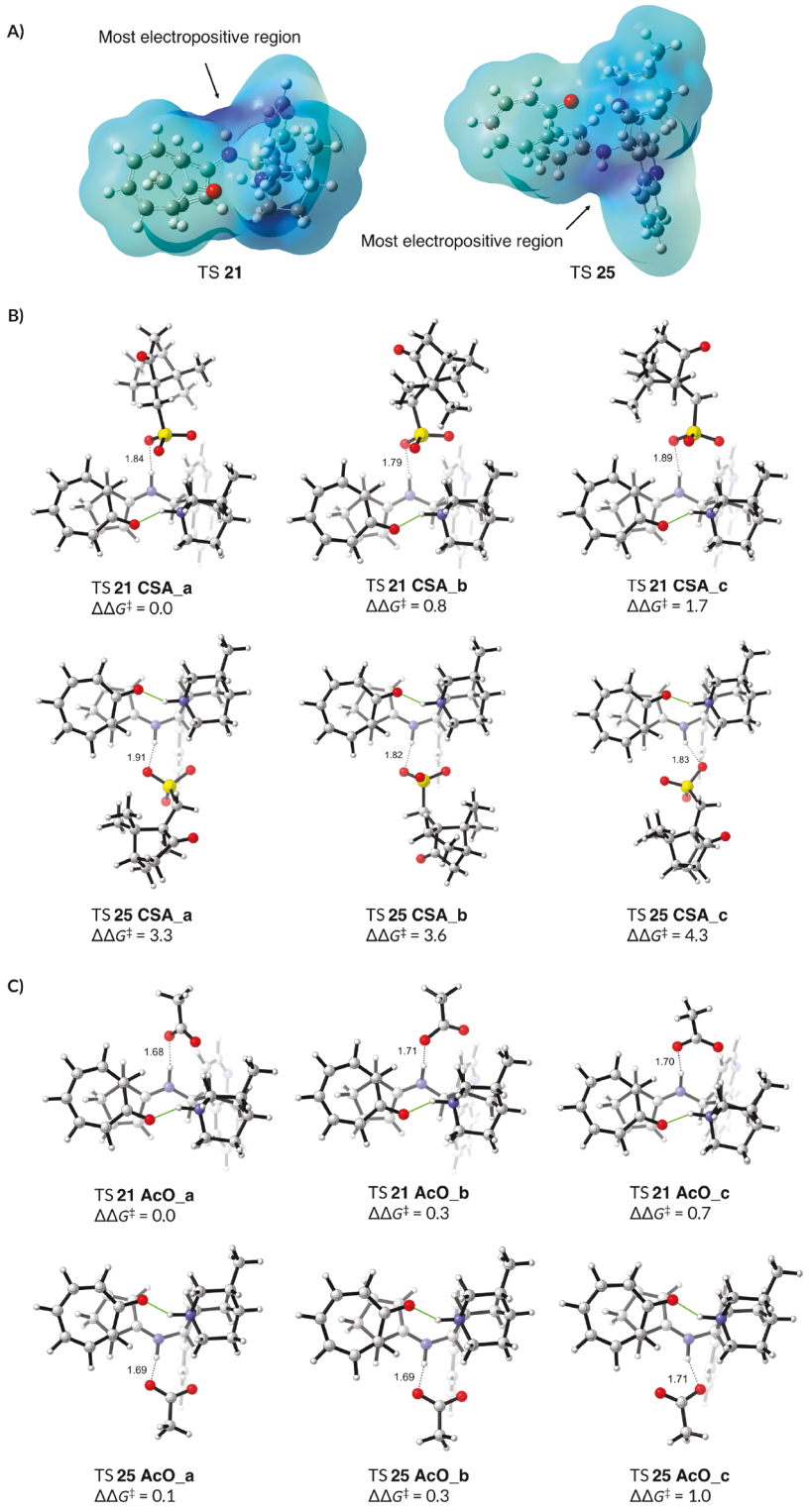

Figure 9. Computational explorations of the counterion effects on the stereoselectivity. (A) Computed electrostatic potential (ESP) maps of TSs **21** and **25**. (B) TSs **21** and **25** with (−)-CSA counterion. (C) TSs **21** and **25** with acetate.

non-cyclic TS structure (see Supporting Information, Figure S8), explaining the low enantioselectivity observed in Table 1, entry 1. The acid is involved in the formation of enamine and the hydrolysis of the enamine from the product as well.

The reaction has also been tested in several solvents (see Supporting Information). In general, high enantioselectivities were observed in non-polar solvents, while the reaction was less enantioselective in polar solvents, such as DMF or MeOH. These observations can be explained by the relative strengths of hydrogen bonds in different solvents. In polar solvents the hydrogen bond between the tropone oxygen atom and the protonated quinuclidinium moiety of the cinchona alkaloid primary amine catalyst **3a** in TS structure **21** is weakened, resulting in a lower enantioselectivity of the reaction. Presumably, reactions can compete via a non-intramolecular hydrogen-bonded TS. In contrast, non-polar solvents strengthen the

DOI: 10.1021/jacs.8b07575
J. Am. Chem. Soc. 2018, 140, 13726−13735

intramolecular hydrogen bond in the TS **21** leading to higher enantioselectivity of the reaction.

We return to the question of the stereoselectivity of the [6+4] cycloaddition between cyclopentenone **1** and tropone **2** catalyzed by the cinchona alkaloid primary amine catalyst **3a**. The stereo-determining TSs are shown in two views in Figure 6A.

TS **21** leading to the major adduct is 1.0 kcal/mol more stable than the TS **25** which leads to the minor adduct. At this stage, a full catalyst model with the vinyl group was also explored and it gave similar results (see Supporting Information). The crown conformer of **21** is distorted in **25**. The difference in energy appears to come from the two hydrogen−hydrogen repulsions from H−H distances of 2.08 and 2.25 Å observed in the TS providing the minor [6+4] cycloaddition adduct. The bottom views of the TSs also suggest a difference in conformation of the cross-dienamine intermediate; the NH-moiety points up in the TS giving the major [6+4] cycloaddition adduct and down in the TS for the less favored adduct. In a different perspective of the TS providing the minor [6+4] cycloaddition adduct (Figure 6B). It is notable, that the 6π- and 4π-components of both TSs are a pair of mirror images. An overlay at the π-components of both TSs is shown. The preference for the *gauche*-(+) conformation is consistent with the one we found in the truncated models.

To understand the intrinsic preference of the cross-dienamine intermediate conformations, the tropone **2** in the enantio-determining TSs was removed, and the remaining cross-dienamine intermediate conformations were optimized (Figure 7).

The energy difference between the two conformations is 0.7 kcal/mol favoring cross-dienamine intermediate **26**, the conformation in the TS for the most favored adduct. The dihedral angle (highlighted in pink) in **27** is −117°, which resembles the *anti-open* conformation of cinchona alkaloids. The same dihedral angle in dienamine **28** is −76°, which is closer to the *syn-open* conformation. By comparing the two cross-dienamine intermediate conformers to the stereo-determining TSs, it is observed that this dihedral angle becomes closer to *anti* (−120°) in the major TS and closer to *syn* (−71°) in the minor TS.

Our hypothesis that the two hydrogen−hydrogen repulsive interactions destabilize the TS for the less favored [6+4] cycloaddition adduct was validated in the truncated model, where the quinoline ring was removed. In the absence of the quinoline, the repulsions are no longer observed, and the enantioselectivity diminishes (Supporting Information, Figure S5).

In our computational model, the catalyst is a truncated version of **3a** used in the experiments, where the vinyl group of **3a** is modeled with a methyl group. Due to the relatively small difference in energy between TSs **21** and **25**, we re-computed the two key TSs with the vinyl group to provide a genuinely exact catalyst model. The results are shown in Figure 8. There are three conformations of the vinyl group (highlighted in green) for each TS. Including the vinyl group does not affect our conclusions on the stereoselectivity.

To further explore the effects of counterion on the stereoselectivity, we re-computed TSs **21** and **25** (cationic) in the presence of negatively charged counterion. At this stage, a full conformational search for ion pairs would be prohibitive. To determine the most probable configurations of the ion pair, we first computed the electrostatic potential (ESP) maps of TSs **21** and **25** (Figure 9A). Then the counterion was placed at the most electropositive region of each TS with a few different orientations. The effects of two different counterions were explored. The TSs with (−)-CSA counterion are shown in Figure 9B, while the TSs with acetate counterion are shown in Figure 9C. The differences in energy between the major and minor TSs are 3.3 and 0.1 kcal/mol for (−)-CSA and acetate, respectively. These results qualitatively reproduce the high selectivity with CSA and lower selectivities with carboxylic acids. However, an extensive conformational search of ion pairs would be needed before any quantitative conclusions can be drawn. Despite being qualitative, the trend observed from these data suggests that the stronger association of carboxylates with the cationic TS may adversely affect the enantioselectivity of the reaction.

CONCLUSIONS

The mechanism and origins of chemo- and stereoselectivities of the organocatalytic [6+4] cycloaddition between 2-cyclopentenone and tropone have been studied with density functional theory computations and further experimental investigations. The [6+4] cycloaddition is a stepwise process, and the [6+4] cycloaddition is much faster than the potentially competing [4+2] cycloaddition. The cross-dienamine intermediate forms in preference to the linear-dienamine intermediate in the presence of the cinchona alkaloid primary amine catalyst and an acid additive. The concentration of the acid additive is important to the good yields and excellent enantioselectivities of the reaction. The rate- and stereo-determining TS structure features a strong hydrogen-bonding interaction between the tropone oxygen and the protonated quinuclidine. Different truncated versions of the system have been investigated to probe the influence of substituents and conformations on the reaction. The enantioselectivity originates from the repulsive hydrogen−hydrogen interactions present in the TS structure that leads to the minor enantiomer.

ASSOCIATED CONTENT

Supporting Information

The Supporting Information is available free of charge on the ACS Publications website at DOI: 10.1021/jacs.8b07575.

Additional computational results; experimental details; coordinates and energies of stationary points (PDF)

AUTHOR INFORMATION

Corresponding Author

*houk@chem.ucla.edu

ORCID

Peiyuan Yu: 0000-0002-4367-6866
Cyndi Qixin He: 0000-0002-3143-6435
Adam Simon: 0000-0001-6334-3359
Karl Anker Jørgensen: 0000-0002-3482-6236
K. N. Houk: 0000-0002-8387-5261

Author Contributions

#P.Y. and C.Q.H. contributed equally.

Notes

The authors declare no competing financial interest.

ACKNOWLEDGMENTS

We are grateful to the National Science Foundation (CHE-1361104 and CHE-1764328) for financial support of this research. Calculations were performed on the Hoffman2 cluster at UCLA and the Extreme Science and Engineering

DOI: 10.1021/jacs.8b07575
J. Am. Chem. Soc. 2018, 140, 13726−13735

Discovery Environment (XSEDE), which is supported by the National Science Foundation (OCI-1053575). R.M., M.K.T. and K.A.J. thank the "Semper Ardens" program of the Carlsberg Foundation and Aarhus University for financial support. A.S. thanks the National Institutes of General Medical Sciences, National Institutes of Health Chemistry-Biology Interface Training Program for support.

REFERENCES

(1) (a) Diels, O.; Alder, K. *Justus Liebigs Ann.* **1928**, *460*, 98. (b) Diels, O.; Alder, K. *Ber. Dtsch. Chem. Ges. B* **1929**, *62*, 554.
(2) See, e.g.: (a) Woodward, R. B.; Bader, F. E.; Bickel, H.; Frey, A. J.; Kierstead, R. W. *J. Am. Chem. Soc.* **1956**, *78*, 2023. (b) Corey, E. J.; Schaaf, T. K.; Huber, W.; Koelliker, U.; Weinshenker, N. M. *J. Am. Chem. Soc.* **1970**, *92*, 397. (c) Maimone, T. J.; Shi, J.; Ashida, S.; Baran, P. S. *J. Am. Chem. Soc.* **2009**, *131*, 17066. (d) Stork, G.; Yamashita, A.; Hanson, R. M.; Phan, L.; Phillips, E.; Dubé, D.; Bos, P. H.; Clark, A. J.; Gough, M.; Greenlee, M. L.; Jiang, Y.; Jones, K.; Kitamura, M.; Leonard, J.; Liu, T.; Parsons, P. J.; Venkatesan, A. M. *Org. Lett.* **2017**, *19*, 5150.
(3) (a) Hoffmann, R.; Woodward, R. B. *J. Am. Chem. Soc.* **1965**, *87*, 2046. (b) Hoffmann, R.; Woodward, R. B. *J. Am. Chem. Soc.* **1965**, *87*, 4388. (c) Woodward, R. B.; Hoffmann, R. *Angew. Chem., Int. Ed. Engl.* **1969**, *8*, 781.
(4) (a) Corey, E. J. *Angew. Chem., Int. Ed.* **2002**, *41*, 1650. (b) Nicolaou, K. C.; Snyder, S. A.; Montagnon, T.; Vassilikogiannakis, G. *Angew. Chem., Int. Ed.* **2002**, *41*, 1668.
(5) (a) Woodward, R. B.; Katz, T. J. *Tetrahedron* **1959**, *5*, 70. (b) Dewar, M. J. S.; Olivella, S.; Stewart, J. J. P. *J. Am. Chem. Soc.* **1986**, *108*, 5771. (c) Goldstein, E.; Beno, B.; Houk, K. N. *J. Am. Chem. Soc.* **1996**, *118*, 6036.
(6) Palazzo, T. A.; Mose, R.; Jørgensen, K. A. *Angew. Chem., Int. Ed.* **2017**, *56*, 10033.
(7) (a) Takeshita, H.; Wada, Y.; Mori, A.; Hatsui. *Chem. Lett.* **1973**, *2*, 335. (b) Dahnke, K. R.; Paquette, L. A. *J. Org. Chem.* **1994**, *59*, 885. (c) Li, P.; Yamamoto, H. *Chem. Commun.* **2010**, *46*, 6294. (d) Li, P.; Yamamoto, H. *J. Am. Chem. Soc.* **2009**, *131*, 16628. (e) Houk, K. N.; Luskus, L. J.; Bhacca, N. S. *J. Am. Chem. Soc.* **1970**, *92*, 6392. (f) Yu, P.; Chen, T. Q.; Yang, Z.; He, C. Q.; Patel, A.; Lam, Y. H.; Liu, C. Y.; Houk, K. N. *J. Am. Chem. Soc.* **2017**, *139*, 8251. (g) Trost, B. M.; Seoane, P. R. *J. Am. Chem. Soc.* **1987**, *109*, 615. (h) Trost, B. M.; McDougall, P. J.; Hartmann, O.; Wathen, P. T. *J. Am. Chem. Soc.* **2008**, *130*, 14960. (i) Trost, B. M.; McDougall, P. J. *Org. Lett.* **2009**, *11*, 3782. (j) Rigby, J. H.; Fleming, M. *Tetrahedron Lett.* **2002**, *43*, 8643. (k) Isakovic, L.; Ashenhurst, J. A.; Gleason, J. L. *Org. Lett.* **2001**, *3*, 4189. (l) Ashenhurst, J. A.; Gleason, J. L. *Tetrahedron Lett.* **2008**, *49*, 504. (m) Ashenhurst, J. A.; Isakovic, L.; Gleason, J. L. *Tetrahedron* **2010**, *66*, 368. (n) Nozoe, T.; Mukai, T.; Osaka, K.; Shishido, N. *Bull. Chem. Soc. Jpn.* **1961**, *34*, 1384. (o) Mukai, T.; Tezuka, T.; Akasaki, Y. *J. Am. Chem. Soc.* **1966**, *88*, 5025. (p) Cantrell, T. S. *J. Am. Chem. Soc.* **1971**, *93*, 2540.
(8) (a) Rigby, J. H.; Rege, S. D.; Sandanayaka, V. P.; Kirova, M. *J. Org. Chem.* **1996**, *61*, 842. See also for a racemic version: (b) Rigby, J. H.; et al. *J. Am. Chem. Soc.* **1993**, *115*, 1382.
(9) (a) Xie, M.; Liu, X.; Wu, X.; Cai, Y.; Lin, L.; Feng, X. *Angew. Chem., Int. Ed.* **2013**, *52*, 5604. (b) Xie, M.; Wu, X.; Wang, G.; Lin, L.; Feng, X. *Huaxue Xuebao* **2014**, *72*, 856.
(10) Garst, M. E.; Roberts, V. A.; Houk, K. N.; Rondan, N. G. *J. Am. Chem. Soc.* **1984**, *106*, 3882.
(11) Mose, R.; Preegel, G.; Larsen, J.; Jakobsen, S.; Iversen, E. H.; Jørgensen, K. A. *Nat. Chem.* **2017**, *9*, 487.
(12) Frisch, M. J.; Trucks, G. W.; Schlegel, H. B.; Scuseria, G. E.; Robb, M. A.; Cheeseman, J. R.; Scalmani, G.; Barone, V.; Mennucci, B.; Petersson, G. A.; Nakatsuji, H.; Caricato, M.; Li, X.; Hratchian, H. P.; Izmaylov, A. F.; Bloino, J.; Zheng, G.; Sonnenberg, J. L.; Hada, M.; Ehara, M.; Toyota, K.; Fukuda, R.; Hasegawa, J.; Ishida, M.; Nakajima, T.; Honda, Y.; Kitao, O.; Nakai, H.; Vreven, T.; Montgomery, J. A., Jr.; Peralta, J. E.; Ogliaro, F.; Bearpark, M.; Heyd, J. J.; Brothers, E.; Kudin, K. N.; Staroverov, V. N.; Kobayashi, R.; Normand, J.; Raghavachari, K.; Rendell, A.; Burant, J. C.; Iyengar, S. S.; Tomasi, J.; Cossi, M.; Rega, N.; Millam, J. M.; Klene, M.; Knox, J. E.; Cross, J. B.; Bakken, V.; Adamo, C.; Jaramillo, J.; Gomperts, R.; Stratmann, R. E.; Yazyev, O.; Austin, A. J.; Cammi, R.; Pomelli, C.; Ochterski, J. W.; Martin, R. L.; Morokuma, K.; Zakrzewski, V. G.; Voth, G. A.; Salvador, P.; Dannenberg, J. J.; Dapprich, S.; Daniels, A. D.; Farkas, O.; Foresman, J. B.; Ortiz, J. V.; Cioslowski, J.; Fox, D. J. *Gaussian 09*, revision D.01; Gaussian, Inc.: Wallingford, CT, 2013.
(13) (a) Lee, C.; Yang, W.; Parr, R. G. *Phys. Rev. B: Condens. Matter Mater. Phys.* **1988**, *37*, 785. (b) Becke, A. D. *J. Chem. Phys.* **1993**, *98*, 5648. (c) Stephens, P. J.; Devlin, F. J.; Chabalowski, C. F.; Frisch, M. J. *J. Phys. Chem.* **1994**, *98*, 11623.
(14) Marenich, A. V.; Cramer, C. J.; Truhlar, D. G. *J. Phys. Chem. B* **2009**, *113*, 6378.
(15) (a) Zhao, Y.; Truhlar, D. G. *Theor. Chem. Acc.* **2008**, *120*, 215. (b) Zhao, Y.; Truhlar, D. G. *Acc. Chem. Res.* **2008**, *41*, 157.
(16) Zhao, Y.; Truhlar, D. G. *Phys. Chem. Chem. Phys.* **2008**, *10*, 2813.
(17) Goldstein, E.; Beno, B. R.; Houk, K. N. *Theor. Chem. Acc.* **1999**, *103*, 81.
(18) Seebach, D.; Golinski, J. *Helv. Chim. Acta* **1981**, *64*, 1413.

DOI: 10.1021/jacs.8b07575
J. Am. Chem. Soc. 2018, 140, 13726−13735